IEEE Access
Multidisciplinary | Rapid Review | Open Access Journal

Received April 14, 2021, accepted April 23, 2021, date of publication May 11, 2021, date of current version May 28, 2021.

Digital Object Identifier 10.1109/ACCESS.2021.3079303

A Time-Varying Sliding Mode Control Method for Distributed-Mass Double Pendulum Bridge Crane With Variable Parameters

TIANLEI WANG[1,2], NANLIN TAN[1], XIANWEN ZHANG[1,2], GUOZHENG LI[1], SHUQIANG SU[1], JING ZHOU[2], JIONGZHI QIU[2], ZHIQIN WU[2], YIKUI ZHAI[2,3], (Member, IEEE), RUGGERO DONIDA LABATI[3], (Member, IEEE), VINCENZO PIURI[3], (Fellow, IEEE), AND FABIO SCOTTI[3], (Member, IEEE)

[1]School of Mechanical, Electronic and Control Engineering, Beijing Jiaotong University, Beijing 100044, China
[2]Department of Intelligent Manufacturing, Wuyi University, Jiangmen 529020, China
[3]Departimento di Information, Universita Degli Studi di Milano, 20133 Milano, Italy

Corresponding author: Tianlei Wang (tianlei.wangi@aliyun.com)

This work was supported in part by the National Natural Science Foundation of China under Grant 51505154 and Grant 51437005, in part by the Science and Technology Project of Jiangmen City under Grant 2019JC01029, Grant 2019JC01005, and Grant 2020JC01035; and in part by the College Students' Innovative Entrepreneurial Training Plan Program under Grant 202011349015S and Grant S202011349041.

ABSTRACT This paper aims to explain the design of a novel time-varying sliding mode control of variable parameter (VP-TVSMC), which can effectively solve the anti-swing and positioning problem of distributed-mass double pendulum bridge crane system with its quick responsiveness and strong robustness to external interference. More specifically, this model initiates with the establishment of the dynamic equation of double pendulum crane model based on distributed-mass, then followed by the design of a time-varying parameter to realize the dynamic adjustment of the sliding mode surface and enhance the adjustment ability of the sliding mode surface, which is conducive to the global robustness of the double pendulum crane system under VP-TVSMC. With Lyapunov method and LaSalle's invariance principle, the asymptotic stability of the system can be sufficiently proved. Finally, the adoption of three kinds of external interference signals and uncertain system parameters successfully verified the preeminent control performance and global robustness against external interference of the proposed controller. The simulation results indicate that compared with the conventional CSMC and PDSMC, the proposed control method can reduce the driving force of the trolley, ensure the rapid and precise positioning of the trolley, as well as restrain the load swing angle within 5° in an effective manner. In addition, compared with the symbolic function sgn(S), the designed continuous function th(S) possesses a better anti-chattering effect, thus strengthening of the control performance of VP-TVSMC.

INDEX TERMS Bridge crane, distributed-mass, time-varying sliding mode control, LaSalle's invariance principle, variable parameter, global robustness.

I. INTRODUCTION

With the advantages of strong transport capacity and high operational flexibility, bridge crane has been extensively applied in modern industrial production [1]–[3]. During transportation, the trolley in the bridge crane system is subject to various interference from the outside world, which may cause the inevitable swinging of the load, unsatisfying working efficiency of the crane system, the possible rolling-off of the load, and ultimately leading to possible serious safety accidents. Therefore, it is of great theoretical significance and engineering practical value to deliberate the control method of the underactuated system so as to achieve the accurate positioning of the bridge crane and minimize the load swing range [4]–[9].

At present, there are mainly two kinds of bridge crane system control methods: open loop control and closed loop control. The former method mainly consists of input shaping [10], [11], optimal control [12], [13] and off-line trajectory planning [14], [15]. In the literature [10] an improved input shaper for the three-dimensional bridge crane system can be located, which is capable of adapting to the change

The associate editor coordinating the review of this manuscript and approving it for publication was Ning Sun.

of cable length and load swing angle in the process of crane transportation. Moreover, N. Sun [12] obtained the optimal energy solution of the bridge crane system control through the optimal control method, which greatly reduced the energy consumption of the system, effectively suppressed the residual oscillation of the load swing angle and achieved a comparatively favorable control effect. In addition, the literature [14] proposed a terminal sliding mode observer to minimize the impact from the possible unknown disturbances of the two-dimensional single pendulum bridge crane system. After that, with a finite time trajectory tracking controller synthesized by using the estimated information, it can be ensured that the system could move along the predetermined trajectory in a finite time. If the system model bears out to be accurate and ideal, the open loop control can undoubtedly achieve better control effect. However, the rareness of the ideal conditions has made closed-loop control with high precision and insensitivity to external disturbance and system parameter changes to be more commonly applied in practical engineering. For this, many domestic and foreign scholars have carried out a lot of researches, such as PID control [16], adaptive control [17], [18], sliding mode control [19]–[21], fuzzy control [22], [5], passive control [23], [24] and online trajectory planning [25], [26]. To be more specific, the literature [16], in order to reduce the errors of vehicle positioning caused by uncertain external disturbances and unmodeled dynamics, expounded a quasi-PID controller without object parameters, which can effectively guarantee the stability of the system. Among them, Lu *et al.* [17] proposed the adaptive output feedback control and applied it to the anti-swing control of the double bridge crane system, which overcame the uncertainty of load quality and thus eliminated the adverse effects of system parameter interference. What's more, the studies of the influence of CSMC and HSMC on the performance of double-pendulum bridge crane system have been demonstrated in the literature [19], with its results to show that both control algorithms can converge asymptotically to the expected value, and in general, CSMC displayed better control effect. Literature [20] combined the advantages of sliding mode control and PD control, and designed an enhanced coupled PD controller based on sliding mode control, whose framework is constructed by using the sliding mode control part, and then the PD control part is used in the stability control system. This method shows robustness to uncertain models, external disturbances and different system parameters. Regarding to the chattering problem of the sliding mode control in the approaching stage, the literature [22] utilized fuzzy control to effectively estimate the uncertainty of the system, and designed a fuzzy sliding mode controller to eliminate chattering phenomenon while the literature [26] proposed an online trajectory planning method in which the trajectory includes a pendulum angle component and a trolley displacement component, whose information was fed back to the designed trajectory in real time through closed-loop control.

To sum up, the research works of scholars have promoted the control technology progress of the bridge crane system to different extent, but this field still requires much more efforts to be optimized. For example, the literature [19], [21], [22] ignored the external uncertain interference in the experimental process, did not ensure the initial time of the system on the expected sliding surface, and lacked the dynamic adjustment of the system while the controller in the literature [25]–[27] featured with complicated design and required high control parameters. On the contrary, the structure of PDSMC controller proposed in the crane is insanely simple and lacks more positioning and swing angle information, which leads to mediocre anti-swing performance [20].

In order to compensate for the shortcomings of the existing researches, we propose a novel time-varying sliding mode controller for the distributed mass double pendulum bridge crane system, which features with simple design and remarkable functions. Meanwhile, a continuous switching function is incorporated for ensuring the continuity of the sliding mode control in the switching process so as to keep the sliding mode control staying on the sliding mode surface in the initial state, which can effectively eliminate the chattering of the sliding mode control. In addition, it is clarified that the design of time-varying parameters in the sliding mode surface is the key to the VP-TVSMC controller, and the design of appropriate sliding mode surface is challenging to maintain the good control performance of the bridge crane. After analyzing the simulation results, it can be confirmed that the new time-varying sliding mode controller can enhance quick and precise localization of the trolley and owns good anti-swing performance and strong robustness to external interference. The main contributions of this paper can be referred to below:

1) Basing on distributed-mass load, the effective double pendulum dynamics model was established. Different from the traditional single pendulum or double pendulum model, the second-order vibration mode of distributed mass load is fully considered in the modeling process, and autobiographical perturbation is introduced, which provides a more accurate dynamic model for the design of the controller.
2) The continuous switching function th(S) designed in this paper, compared with the discontinuous sign function sgn(S), can facilitate a good anti-chattering effect in the double pendulum crane system and enhance the control performance of VP-TVSMC.
3) Compared with the closed-loop control CSMC and PDSMC of the double pendulum crane, the VP-TVSMC designed in this paper has strong robustness, high system stability and sound load swinging suppression performance, which are all conducive to the improvement of the overall control performance.

The other sections of this paper are arranged as follows: Section 1 describes the double pendulum model of the bridge crane system based on distributed mass; Section 2 elaborates the new time-varying sliding mode controller proposed in this paper. After analyzing the stability of the controller in section 3; section 4 verifies the control performance and anti-interference ability of the new

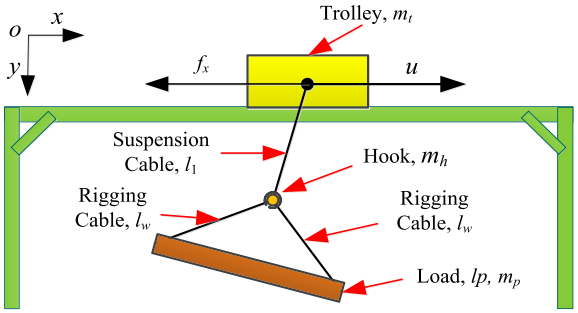

FIGURE 1. Physical model of distributed mass load movement.

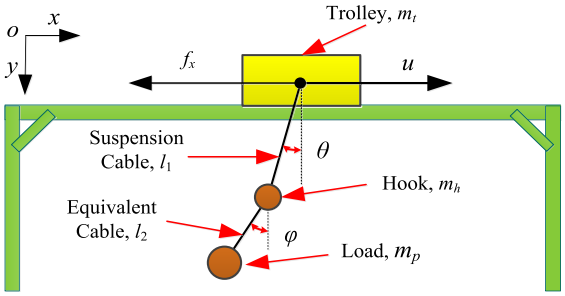

FIGURE 2. Double pendulum physical model of bridge crane system.

time-varying sliding mode controller by experiments on Simulink; Finally, Section 5 provides the summary and prospect of the main work of this paper.

II. DOUBLE PENDULUM DYNAMICS OF BRIDGE CRANE SYSTEM

When steel is transported by bridge crane, as shown in Fig. 1, the connection between the hook and the steel rope remains fixed, and the two steel ropes between the hook and the steel share the same length as l_w so as to prevent the tipping accident of the steel caused by the sliding of the steel rope. The load length is l_p. Since the mass of steel is evenly distributed, the center of mass can be utilized to represent the total mass of steel; that is, the center of steel. Then according to the midline theorem, the equivalent rope length l_2 of the hook and the center of mass of the steel can be easily obtained. Therefore, the double pendulum physical model for the bridge crane system can be established showed in Fig. 2.

On the double pendulum model for the bridge crane system, we build a rectangular coordinate system, in which the positive direction of the X axis follows the power direction, the positive direction of the Y axis points to the vertical ground downward; thus the coordinates of the trolley, the hook and the load can be regarded as(x, y_0), (x_1, y_1), (x_2, y_2) while the mass of the trolley, hook and load can be denoted as m_t, m_h and m_p respectively. The trolley and the lifting hook are connected by steel wire rope whose length is l_1, while the equivalent rope length of the lifting hook and the load is l_2. In the trolley movement process, the friction force of the rail is marked as f_x and the driving force of the motor as u. The generalized coordinates of the system are arranged as follows: horizontal displacement x of the trolley, the first pendulum angle θ, and the second pendulum angle φ, so the double pendulum model of the bridge crane system under the generalized coordinates can be established as demonstrated in Fig. 2.

In this paper, the load is considered as a distributed mass with translational and oscillating moment of inertia effects on two axes. Furthermore, it is assumed that the distributed load is suspended on a hook with significant mass, and the load can swing freely. What's more, the hook is modeled as a lumped mass so that its two-dimensional translational inertial effects can be taken into account. The total kinetic energy of the bridge crane system mainly includes the kinetic energy of the trolley, the hook as well as the load, and the specific expression for this can be worked out as follows:

$$\begin{aligned} E_k = &\frac{1}{2}m_t\dot{x}^2 + \frac{1}{2}m_h\left(\dot{x} - l_1\cos\theta\dot{\theta}\right)^2 + \frac{1}{2}m_h\left(l_1\sin\theta\dot{\theta}\right)^2 \\ &+\frac{1}{2}m_p\left(\dot{x} - l_1\cos\theta\dot{\theta} - l_2\cos\varphi\dot{\varphi}\right)^2 \\ &+\frac{1}{2}m_p\left(l_1\sin\theta\dot{\theta} + l_2\sin\varphi\dot{\varphi}\right)^2 + E_w \end{aligned} \tag{1}$$

where, $E_w = \frac{1}{2}J\dot{\varphi}^2$ is autobiographical perturbation kinetic energy.

The moment of inertia is $J = \frac{1}{12}m_p l_p^2$.

The potential energy of the bridge crane system is:

$$E_p = m_h g l_1\left(1 - \cos\theta\right) + m_p g\begin{pmatrix} l_1 - l_1\cos\theta + \\ l_2 - l_2\cos\varphi \end{pmatrix} \tag{2}$$

According to the Lagrange equation, in three generalized coordinates of the horizontal displacement x, the first swing angle θ, and the second swing angle φ of the trolley, the system dynamics equation can be obtained as:

$$\begin{aligned} &\left(m_t + m_h + m_p\right)\ddot{x} - \left(m_h + m_p\right)l_1\cos\theta\ddot{\theta} \\ &\quad -m_p l_2\cos\varphi\ddot{\varphi} + \left(m_h + m_p\right)l_1\sin\theta\dot{\theta}^2 \\ &\quad +m_p l_2\sin\varphi\dot{\varphi}^2 = u - f_x \end{aligned} \tag{3}$$

$$\begin{aligned} &-\left(m_h + m_p\right)l_1\cos\theta\ddot{x} + \left(m_h + m_p\right)l_1^2\ddot{\theta} \\ &\quad +m_p l_1 l_2\cos(\theta - \varphi)\ddot{\varphi} + m_p l_1 l_2\sin(\theta - \varphi)\dot{\varphi}^2 \\ &\quad +\left(m_h + m_p\right)g l_1\sin\theta = 0 \end{aligned} \tag{4}$$

$$\begin{aligned} &-m_p l_2\cos\varphi\ddot{x} + m_p l_1 l_2\cos(\theta - \varphi)\ddot{\theta} + m_p\left(l_2^2 + \frac{1}{12}l_p^2\right)\ddot{\varphi} \\ &\quad -m_p l_1 l_2\sin(\theta - \varphi)\dot{\theta}^2 + m_p g l_2\sin\varphi = 0 \end{aligned} \tag{5}$$

For the bridge crane system, the friction force of the trolley is nonlinear and related to the trolley speed. The speed and friction data of the trolley were obtained through the experiment, and then the functions close to the experimental data were selected for data fitting [27]. So we choose to adopt the following friction model of the system:

$$f_x = f_r\tanh\left(\dot{x}/\varepsilon_x\right) - k_{rx}\left|\dot{x}\right|\dot{x} \tag{6}$$

where, $f_r, \varepsilon_x, k_{rx} \in \mathrm{R}$ are the corresponding friction factor.

Equations (3), (4) and (5) are rewritten into matrix form as follows:

$$\boldsymbol{M}(\boldsymbol{q})\ddot{\boldsymbol{q}} + \boldsymbol{C}(\boldsymbol{q}, \dot{\boldsymbol{q}})\dot{\boldsymbol{q}} + \boldsymbol{G}(\boldsymbol{q}) = \boldsymbol{U} + \boldsymbol{d}_f \tag{7}$$

where, $\boldsymbol{M}(\boldsymbol{q}) \in \mathrm{R}^{3\times3}$, $\boldsymbol{C}(\boldsymbol{q}, \dot{\boldsymbol{q}}) \in \mathrm{R}^{3\times3}$, $\boldsymbol{G}(\boldsymbol{q}) \in \mathrm{R}^{3\times1}$ are respectively expressed as inertia matrix, Centripetal-Coriolis force matrix and gravity matrix, and the driving force and resistance of the system are respectively indicated by $\boldsymbol{U} \in \mathrm{R}^3$, $\boldsymbol{d}_f \in \mathrm{R}^3$. Equation (8) can be referred to the state of the bridge crane system:

$$\boldsymbol{q} = [x \quad \theta \quad \varphi]^{\mathrm{T}} \tag{8}$$

The inertia matrix $\boldsymbol{M}(\boldsymbol{q}) \in \mathrm{R}^{3\times3}$ belongs to symmetric matrix:

$$\boldsymbol{M}(\boldsymbol{q}) = \begin{bmatrix} m_{11} & m_{12} & m_{13} \\ m_{21} & m_{22} & m_{23} \\ m_{31} & m_{32} & m_{33} \end{bmatrix} \tag{9}$$

Centripetal-Coriolis force matrix $\boldsymbol{C}(\boldsymbol{q}, \dot{\boldsymbol{q}}) \in \mathrm{R}^{3\times3}$ is:

$$\boldsymbol{C}(\boldsymbol{q}, \dot{\boldsymbol{q}}) = \begin{bmatrix} 0 & c_{12} & c_{13} \\ 0 & 0 & c_{23} \\ 0 & c_{32} & 0 \end{bmatrix} \tag{10}$$

The gravity matrix $\boldsymbol{G}$ refers to:

$$\boldsymbol{G} = [0 \; g_2 \; g_3]^{\mathrm{T}} \tag{11}$$

The driving force $\boldsymbol{U} \in \mathrm{R}^3$ works as:

$$\boldsymbol{U} = [u \; 0 \; 0]^{\mathrm{T}} \tag{12}$$

The interference resistance $\boldsymbol{d}_f \in \mathrm{R}^3$ is:

$$\boldsymbol{d}_f = [-f_x \; 0 \; 0]^{\mathrm{T}} \tag{13}$$

where, the specific expression of each item of equations (9)-(11) can be written as:

$$\begin{aligned}
m_{11} &= m_t + m_h + m_p, m_{12} = -\left(m_h + m_p\right) l_1 \cos\theta \\
m_{13} &= -m_p l_2 \cos\varphi, m_{21} = -\left(m_h + m_p\right) l_1 \cos\theta \\
m_{22} &= \left(m_h + m_p\right) l_1^2, m_{23} = m_p l_1 l_2 \cos\left(\theta - \varphi\right) \\
m_{31} &= -m_p l_2 cos\varphi, m_{32} = m_p l_1 l_2 \cos\left(\theta - \varphi\right) \\
m_{33} &= m_p(l_2^2 + \frac{1}{12} l_p^2), c_{12} = \left(m_h + m_p\right) l_1 \sin\theta\dot{\theta} \\
c_{13} &= m_p l_2 \sin\varphi\dot{\varphi}, c_{23} = m_p l_1 l_2 \sin\left(\theta - \varphi\right)\dot{\varphi}, \\
g_3 &= m_p g l_2 \sin\varphi, c_{32} = -m_p l_1 l_2 \sin\left(\theta - \varphi\right)\dot{\theta}, \\
g_2 &= \left(m_h + m_p\right) g l_1 \sin\theta
\end{aligned}$$

Remark 1: The unknown disturbance matrix $\boldsymbol{d}_f$ as a differentiable function with position derivative x, mainly describes the external resistance of the system, which shows a nonlinear relationship with the trolley displacement x and the trolley velocity $\dot{x}$. In the process of trolley movement, without considering the elasticity of the cable, which means that rope length stays the same during calculation, we can have $\dot{l}_i \equiv 0, i = 1, 2$. In this paper, it has been mentioned that the trolley mass m_t, the load mass m_p, the hook mass m_h, the cable length l_1 and l_2 are all nominal values. Consequently, so as to facilitate the design of the sliding mode controller and the stability proof of the bridge crane system, the following assumptions are made:

Assumption 1: The swing range of load swing angle and hook swing angle are [27]:

$$-\frac{\pi}{2} < \theta < \frac{\pi}{2}, -\frac{\pi}{2} < \varphi < \frac{\pi}{2}$$

According to the dynamic equation (7), the distributed mass based double pendulum bridge crane system only characterizes with one control input but three degrees of freedom, which obviously proves itself as a typical underactuated system. Normally, three degrees of freedom controlled by driving force u, such as carriage displacement x, load swing angle φ and hook swing angle θ, can greatly raises the control difficulty of the system. And either single pendulum crane system or double pendulum crane system shares the same control goals including rapid and pinpoint car positioning and double pendulum suppression. In order to realize these goals, we will design a new controller based on the advantages of time-varying sliding mode control, such as quick response and strong robustness.

III. DESIGN OF VP-TVSMC FOR BRIDGE CRANE SYSTEM

A. CONTROLLER DESIGN SCHEME

For keeping the bridge crane system on the sliding mode surface, a time-varying sliding mode controller with variable parameters (VP-TVSMC) is designed in this paper, whose design process can be located below. This design mainly serves to reduce the chattering of the crane and enhance the robustness of the crane system.

Seen from Fig. 3, the whole control framework is composed of four parts: deviation signal design, sliding mode surface construction, time-varying sliding mode controller with variable parameters, and double pendulum crane system with distributed mass. First of all, the deviation signal is designed according to the desired position required. After that, a new time-varying sliding mode surface is constructed by utilizing the deviation signals, for which a time-varying parameter $C(t)$ and a time-varying function $f(t)$ are designed. Afterwards, the driving force of the system can be reached by combining the exponential sliding mode control with the new time-varying sliding mode surface. Lastly, the designed controller is employed to control the distributed mass double pendulum bridge crane system under external wind disturbance and system parameter interference. This process will be expounded in the following paragraphs.

B. CONTROLLER DESIGN

The state quantity of the system denotes as $\boldsymbol{q} = [x \;\; \theta \;\; \varphi]^{\mathrm{T}}$ in equation (8). Then, according to the control objective of the system, it can be known that the expected value of the crane system is:

$$\boldsymbol{q}_{\mathrm{d}} = [x_{\mathrm{d}} \; 0 \; 0]^{\mathrm{T}} \tag{14}$$

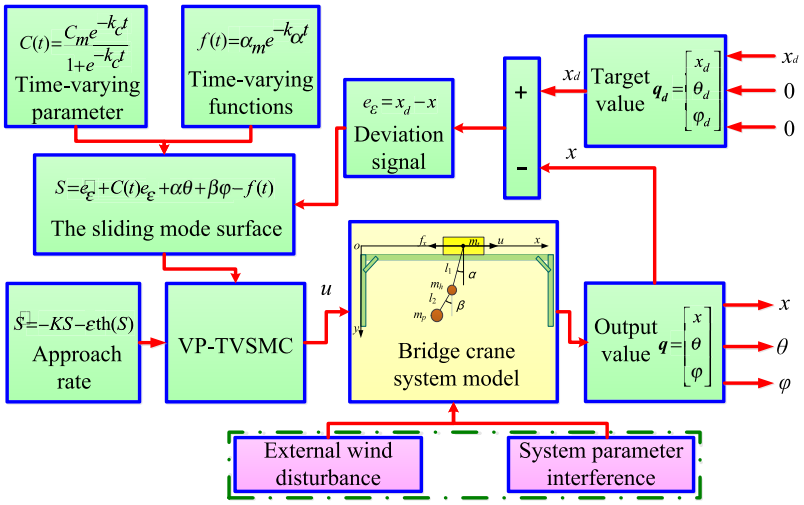

FIGURE 3. VP-TVSMC design flow char.

Next, according to equations (8) and (15), the deviation signal of the designed system is:

$$e_\varepsilon = x_d - x \tag{15}$$

A new time-varying sliding mode surface is arranged for state quantity x, θ, φ of distributed mass double pendulum bridge crane system:

$$S = \dot{e_\varepsilon} + C(t)e_\varepsilon + \alpha\theta + \beta\varphi - f(t) \tag{16}$$

where, $C(t)$ and $f(t)$ are continuous functions of time and first-order differentiable and bounded while α and β denote control gains. What's more, functions $C(t)$ and $f\ (t)$ satisfy the following conditions:

$$C\ (0) = C_0,\ C_\infty = C_n,\ f\ (0) = x_\mathrm{d}C\ (0)\ ,\ f\ (\infty) = 0 \tag{17}$$

where, C_0, C_n and x_d are target constants.

Then we set the continuous, first-order differentiable functions $C(t)$ and $f\ (t)$ as:

$$C\ (t) = \frac{C_m \mathrm{e}^{-k_c t}}{1 + \mathrm{e}^{-k_c t}},\quad f\ (t) = \alpha_m \mathrm{e}^{-k_\alpha t} \tag{18}$$

where, k_c, k_α, C_m, α_m are undetermined constants and $k_c \geq 0$, $k_\alpha \geq 0$, indicating the change rate of continuous functions $C(t)$ and $f\ (t)$. Thus, we can get:

$$S = \dot{e_\varepsilon} + \frac{C_m \mathrm{e}^{-k_c t}}{1 + \mathrm{e}^{-k_c t}} e_\varepsilon + \alpha\theta + \beta\theta - \alpha_m \mathrm{e}^{-k_\alpha t} \tag{19}$$

At the initial moment, $q_0 = [0\ 0\ 0]^\mathrm{T}$ and $S\ (0) = 0$, and equation (20) can be obtained based on equation (19):

$$C_m x_d = 2\alpha_m \tag{20}$$

Take $C_m = \frac{1}{2}$ to get $\alpha_m = \frac{x_\mathrm{d}}{4}$. Therefore, the expressions of functions $C(t)$ and $f\ (t)$ are:

$$C\ (t) = \frac{\mathrm{e}^{-k_c t}}{2\left(1 + \mathrm{e}^{-k_c t}\right)},\quad f\ (t) = \frac{x_d}{4}\mathrm{e}^{-k_\alpha t} \tag{21}$$

Substituting equation (21) into equation (19), we can obtain:

$$S = \dot{e_\varepsilon} + \frac{\mathrm{e}^{-k_c t}}{2\left(1 + \mathrm{e}^{-k_c t}\right)} e_\varepsilon + \alpha\theta + \beta\varphi + \frac{x_\mathrm{d}}{4}\mathrm{e}^{-k_\alpha t} \tag{22}$$

Then the first derivative of equation (22) with respect to time can be obtained as follows:

$$\dot{S} = -\ddot{x} - \frac{k_c \mathrm{e}^{k_i t}}{2\left(1 + \mathrm{e}^{k_\varepsilon t}\right)^2}(x_\mathrm{d} - x) - \frac{\mathrm{e}^{-k_c t}}{2\left(1 + \mathrm{e}^{-k_c t}\right)}\dot{x} + \alpha\dot{\theta} + \beta\dot{\varphi} + \frac{x_\mathrm{d} k_\alpha}{4}\mathrm{e}^{-k_\alpha t} \tag{23}$$

Afterwards, the sliding mode surface will be approached exponentially for the purpose of suppressing the chattering problem of the crane system and quickly reaching the target value, whose detailed expression can be written as:

$$\dot{S} = -KS - \varepsilon\ \mathrm{th}(S) \tag{24}$$

Among which, K and ε are positive SMC gains, while $\mathrm{th}(S)$ is a smooth function, with its main form expressed as follows:

$$\mathrm{th}\ (S) = \begin{cases} 1 - \dfrac{2}{\mathrm{e}^2 + 1}, & S \geq 1 \\ \dfrac{\mathrm{e}^s - \mathrm{e}^{-s}}{\mathrm{e}^s + \mathrm{e}^{-s}}, & |S| < 1 \\ -1 + \dfrac{2}{\mathrm{e}^2 + 1}, & S \leq -1 \end{cases} \tag{25}$$

Since equation (23) equals to equation (24), the formula of trolley acceleration $\ddot{x}$ can be evinced as:

$$\ddot{x} = -\frac{k_c \mathrm{e}^{k_c t}}{2\left(1 + \mathrm{e}^{k_c t}\right)^2}(x_\mathrm{d} - x) - \frac{\mathrm{e}^{-k_c t}}{2\left(1 + \mathrm{e}^{-k_c t}\right)}\dot{x} + \alpha\dot{\theta} + \beta\dot{\varphi} + \frac{x_\mathrm{d} k_\alpha}{4}\mathrm{e}^{-k_\alpha t} + KS + \varepsilon\ \mathrm{th}(S) \tag{26}$$

Then, after the substitution of equation (26) into equation (3), the expression of control force u can be

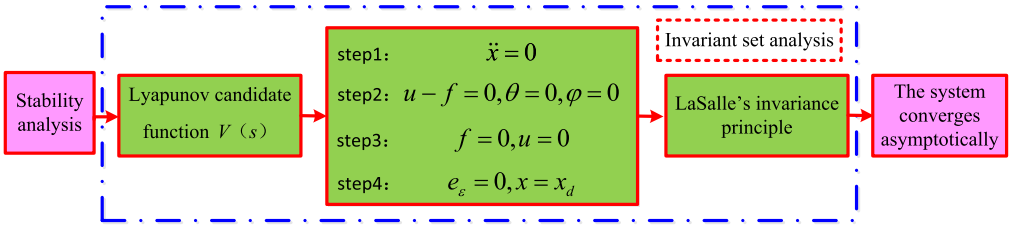

FIGURE 4. Block diagram for proving Theorem.

worked out as:

$$\begin{aligned} u = &\left(m_t + m_h + m_p\right) \\ &\times \begin{bmatrix} -\frac{k_c e^{k_c t}}{2\left(1+e^{k_c t}\right)^2}\left(x_{\mathrm{d}} - x\right) - \frac{e^{-k_c t}}{2\left(1+e^{-k_c t}\right)}\dot{x} \\ +\alpha\dot{\theta} + \beta\dot{\varphi} + \frac{x_{\mathrm{d}} k_\alpha}{4} e^{-k_a t} + KS + \varepsilon\,\mathrm{th}(S) \end{bmatrix} \\ &- \left(m_h + m_p\right) l_1 \cos\theta\ddot{\theta} - m_p l_2 \cos\varphi\ddot{\varphi} \\ &+ \left(m_h + m_p\right) l_1 \sin\theta\dot{\theta}^2 + m_2 l_2 \sin\varphi\dot{\varphi}^2 + f_x \end{aligned} \tag{27}$$

After a series of sliding mode surface design and related algebraic operations, we can receive the driving force u of the double pendulum crane system. The controller contains that high-order feedback information of two state variables: θ and φ, which is beneficial to the control of the system with the growth of the control information in the system. In addition, the proposed controller can realize rapid and precise positioning as well as favorable swing angle suppression under the adjustment of dynamic parameters of time-varying sliding mode surface. Next, the analysis of the proposed VP-TVSMC stability will be conducted.

C. STABILITY ANALYSIS

Theorem 1: For the double pendulum bridge crane system (3), (4) and (5) based on distributed mass, the controller (27) designed in this paper can sustain asymptotic stability at the expected equilibrium point, whose mathematical expression can be written as:

$$\lim_{t\to\infty}\left[x, \dot{x}, \theta, \dot{\theta}, \varphi, \dot{\varphi}\right]^{\mathrm{T}} = \left[x_d, 0, 0, 0, 0, 0\right]^{\mathrm{T}} \tag{28}$$

Proof: The block diagram for the proof is given in Fig. 4. To begin with, we design Lyapunov candidate function as:

$$V = \frac{1}{2}S^2 + K_\delta\left[\frac{\pi}{2} - \arctan\left(\int_0^t \left(\dot{\theta}^2 + \dot{\varphi}^2 + e_\varepsilon^2\right) d\tau\right)\right] \tag{29}$$

where, K_δ pertains to be a positive definite parameter and yet to be determined. It is worth pointing out that $V(t)$ is actually non-negative, and therefore becomes a reasonable candidate for the Lyapunov function, which will be elaborated later. Then, the first derivative of equation (29) can be written as:

$$\dot{V} = S\dot{S} - K_\delta \frac{\dot{\theta}^2 + \dot{\varphi}^2 + e_\varepsilon^2}{1 + \left[\int_0^t \left(\dot{\theta}^2 + \dot{\varphi}^2 + e_\varepsilon^2\right) d\tau\right]^2} \tag{30}$$

Substitute equation (24) into equation (30) to receive:

$$\begin{aligned} \dot{V} &= S\left(-KS - \varepsilon\,\mathrm{th}\left(s\right)\right) - K_\delta \frac{\dot{\theta}^2 + \dot{\varphi}^2 + e_\varepsilon^2}{1 + \left[\int_0^t \left(\dot{\theta}^2 + \dot{\varphi}^2 + e_\varepsilon^2\right) d\tau\right]^2} \\ &= -KS^2 - \varepsilon S\,\mathrm{th}\left(s\right) - K_\delta \frac{\dot{\theta}^2 + \dot{\varphi}^2 + e_\varepsilon^2}{1 + \left[\int_0^t \left(\dot{\theta}^2 + \dot{\varphi}^2 + e_\varepsilon^2\right) d\tau\right]^2} \end{aligned} \tag{31}$$

It can be clearly derived from equation (31) that:

$$-KS^2 \le 0\,,\quad -K_\delta \frac{\dot{\theta}^2 + \dot{\varphi}^2 + e_\varepsilon^2}{1 + \left[\int_0^t \left(\dot{\theta}^2 + \dot{\varphi}^2 + e_\varepsilon^2\right) d\tau\right]^2} \le 0 \tag{32}$$

Subsequently, the symbol of $S\mathrm{th}\left(S\right)$ will be judged. According to equation (25), we can acquire:

$$S\mathrm{th}\left(S\right) = \begin{cases} S(1 - \frac{2}{e^2+1}), & S \ge 1 \\ S\frac{e^S - e^{-S}}{e^S + e^{-S}}, & |S| < 1 \\ -S(1 - \frac{2}{e^2+1}), & S \le -1 \end{cases} \Rightarrow S\mathrm{th}\left(S\right) \ge 0 \tag{33}$$

Then after combining equation (32) and equation (33) to get $\dot{V} \le 0$, it can be observed that Lyapunov function gradually decreases with the passage of time. And since $\frac{1}{2}S^2$, $K_\delta\left[\frac{\pi}{2} - arctan\left(\int_0^t \left(\dot{\theta}^2 + \dot{\varphi}^2 + e_\varepsilon^2\right) d\tau\right)\right]$ is positive, the Lyapunov candidate function $V(t)$ is also positive definite and meanwhile $0 \le V(t) \le V(0)$, from which we know that $V(t)$ is bounded. Then, from equation (22) and (29), we can obtain:

$$x, \dot{x}, \theta, \dot{\theta}, \varphi, \dot{\varphi}, e_\varepsilon, \dot{e}_\varepsilon, S, \dot{S} \in \mathrm{L}_\infty \tag{34}$$

To further prove Theorem 1, it would be required to first define the invariant set:

$$\Omega = \left\{S, q | \dot{V}\left(t\right) = 0\right\} \tag{35}$$

It can be inferred from equation (31) and (34) that:

$$S, \dot{\theta}, \dot{\varphi}, e_\varepsilon = 0 \Rightarrow \dot{S}, \ddot{\theta}, \ddot{\varphi}, \dot{e}_\varepsilon = 0 \tag{36}$$

When $t \to \infty$, we get that:

$$S = \dot{x} + \alpha\theta + \beta\varphi, \dot{S} = \ddot{x} + \alpha\dot{\theta} + \beta\dot{\varphi}$$

Then combined with equation (36), it can be further deduced as:

$$\begin{aligned} S &= \dot{x} + \alpha\theta + \beta\varphi = 0, \quad \dot{S} = \ddot{x} + \alpha\dot{\theta} + \beta\dot{\varphi} = 0 \\ &\Rightarrow \dot{x} = -\alpha\theta - \beta\varphi, \ddot{x} = 0 \end{aligned} \tag{37}$$

Then, equation (36) and (37) are substituted into equation (3), (4) and (5) of the double pendulum bridge crane system, and the equations below can be figured out:

$$\begin{cases} u - f_x = 0 \\ \left(m_h + m_p\right) g l_1 \sin\theta = 0 \\ m_p g l_2 \sin\varphi = 0 \end{cases} , \Rightarrow u - f_x = 0, \theta = 0, \varphi = 0 \tag{38}$$

After positioning $\theta = 0, \varphi = 0$ into equation (37), the result of $\dot{x} = 0$ came out. Consequently friction can be written as $f_x = f_r \tanh\left(\dot{x}/\varepsilon_x\right) - k_{rx}|\dot{x}|\dot{x} = 0$, and the driving force as $u = 0$. Moreover, in equation (36) $e_\varepsilon = 0$. In other words, the car position x will eventually converge to the expected value x_d. By summarizing the results of (36), (37) and (38), it is concluded that the maximum invariant set M only contains the expected equilibrium point. Therefore, on the basis of the LaSalle's invariance principle, the closed-loop system turns out to be asymptotically stable near the desired equilibrium point, fully proving theorem 1.

For the next step, the designed controller will need to carry out 5 groups of simulation experiments on the double pendulum bridge crane system.

IV. SIMULATION RESULTS AND ANALYSIS

To inspect the effectiveness, stability and robustness of VP-TVSMC to the control of the double pendulum bridge crane system, relevant simulation experiments have been conducted under the Simulink simulation environment. During the experiments, the system parameters of the bridge crane are: the mass of the trolley $m_t = 50$ kg, the mass of the hook $m_h = 2$ kg, the load mass $m_p = 10$ kg, the gravitational acceleration $g = 9.8$ m/s^2, the connecting rope length of the trolley and the hook $l_1 = 3$ m, the connecting rope length of the hook and the load $l_2 = 0.3$ m, the load $l_p = 0.5$ m, the initial position of the trolley as 0 m, and the expected position as 4 m. The friction parameters between the trolley and the rail are [27]: $f_r = 4.4$, $\varepsilon_x = 0.01$, $k_{rx} = -0.5$.

In order to better reflect the advantages of the VP-TVSMC method proposed in this paper, we primarily compared it with the CSMC method [19] and PDSMC method [20], and then tested the anti-chattering performance of the proposed continuous function th(S) against VP-TVSMC. At length, the robustness of the proposed method against external disturbances and the robustness of the system's uncertain parameters are tested.

Experiment 1: In this group of experiments, the control effects of the proposed method and the existing method

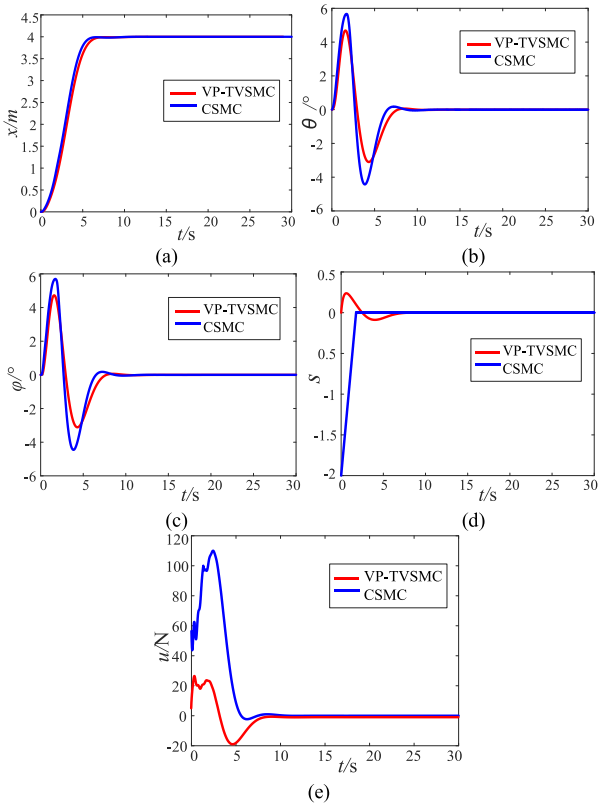

FIGURE 5. State quantity curve of double pendulum bridge crane system.

TABLE 1. VP-TVSMC parameter table.

Symbols for quantities	parameter values	Symbols for quantities	parameter values
K	4	a	-12.4
ε	0.35	β	7
K_c	0.6	x_d	4
K_α	0.75	—	—

CSMC and PDSMC are compared through simulation experiments.

1) CSMC method

$$\begin{aligned} u = &-(m_t + m_h + m_p)(\gamma_1\dot{x} + \alpha_1\dot{\theta} + \beta_1\dot{\varphi}) \\ &- (m_h + m_p)l_1\cos\theta\ddot{\theta} - m_p l_2\cos\varphi\ddot{\varphi} \\ &+ (m_h + m_p)l_1\sin\theta\dot{\theta}^2 + m_2 l_2\sin\varphi\dot{\varphi}^2 + f_x - Ksat(s) \end{aligned} \tag{39}$$

where, $\gamma_1 = 0.5, \alpha_1 = 17, \beta_1 = -1, K = 70$, and the saturation function $sat(s)$ is adopted for the control rate.

2) PDSMC method

$$u = -k_p e - k_d\dot{e} - H\tanh(\dot{e} + \lambda e) \tag{40}$$

where $e = x - x_d + l_1\theta + l_2\varphi$ and $\dot{e} = \dot{x} + l_1\dot{\theta} + l_2\dot{\varphi}$. $k_p = 4.5$, $k_d = 1.5$ are PD control gains, $H = 49$ is the SMC control gain, and $\lambda = 0.3$ is the slide surface slope constant. In the simulation experiments, VP-TVSMC parameters are controlled as shown in Table 1:

With the results demonstrated in Fig. 5, it can be observed that two sliding mode control methods can quickly realize load anti-swinging and positioning, which means when the

carriage displacement is 4 m, both the first and second swing angles can be suppressed effectively. From Fig.5, we can conclude: ① Fig.5(a) shows that under the action of VP-TVSMC control method, CSMC control method and PDSMC control method, the trolley almost arrives at the expected position at the same time in 7s, so the three methods have no obvious difference in the position control effect of the trolley; ② On the aspect of anti-swing performance, VP-TVSMC has a better effect on suppressing swing angle, which can be supported by Fig.5(b) and Fig.5(c) to show that VP-TVSMC outperforms in pendulum angle control because the amplitude of the first and second pendulum angles remains less than 5°. However, under the control of CSMC, both the first and second swing angles are close to 6°, whose difference of control swing angles reaches about 1°. Compared with the above two methods, the PDSMC control method has no significant anti-swing effect on the double pendulum crane system with distributed mass, and the maximum angle of the first pendulum angle and the second pendulum angle is about 5.5°. In addition, there is significant residual chattering at the first and second pendulum angles; ③ Fig.5(d) tells that the sliding surface of VP-TVSMC stays on the sliding surface from the beginning, while the sliding surface of CSMC begins to slide from -2 and the sliding surface of PDSMC begins to slide from -1.2; ④ Fig.5(e) shows that VP-TVSMC defeats CSMC and PDSMC in terms of motor safety guarantee, which greatly lessens the requirement for motor output force.

Experiment 2: Under the same experimental environment, the control effect of continuous function th(S) and symbolic function sgn(S) in equation (28) on VP-TVSMC method is tested, in which the control gain stays the same as that in Table 1 and the experimental results are depicted in Fig.6.

According to the simulation results in Figs.6(a), (b) and (c), continuous function th(S) has a better performance in terms of pallet position and load swing angle, which speeds up the convergence time of pallet position and lessens the amplitude of load swing angle to a certain degree. We can draw from Fig.6(d) that the discontinuity of the sign function sgn(S) gives the sliding mode surface switch a high frequency, while the continuous function th(S) does the total opposite. After further analysis of Fig.6(e), it can be noticed that under the action of the sign function sgn(S), the driving force switches at a high frequency, and the maximum input force reaches 45N. In addition, at about 10s, the driving force oscillates at an equal amplitude of $\pm 19N$. Thus, the continuous function th(S) can not only effectively eliminate the high-frequency switching, but also reduce the output peak value of the driving force, which can effectively reduce further the peak value to about 38N, that is, to achieve a more favourable control effect, as well as to prevent the motor from burning out resulted from frequent positive and negative turnings.

Experiment 3: During transportation, it is easy for a bridge crane to be disturbed by external wind force or strikes, etc., leading to unexpected load shaking. Objectives of this experiment: (1) To verify the robustness of VP-TVSMC.

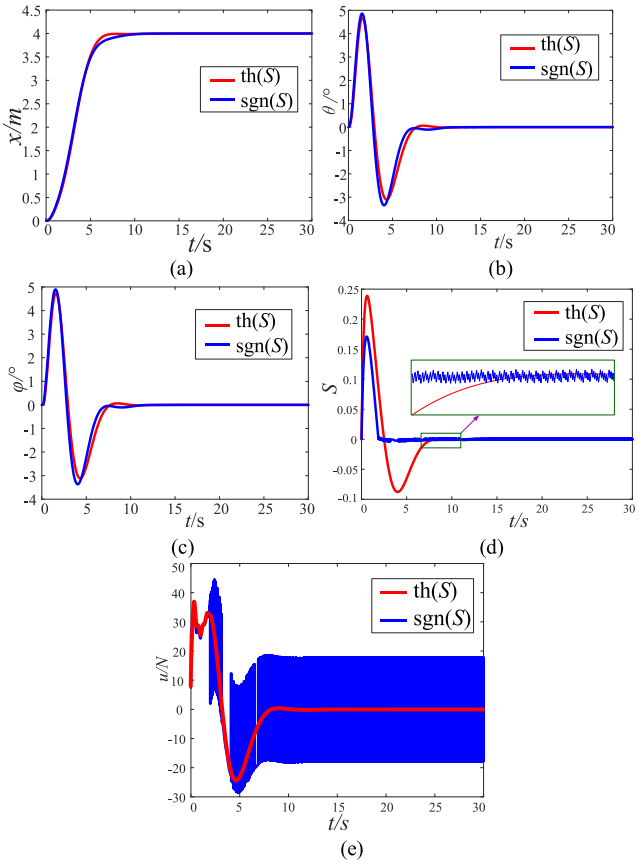

FIGURE 6. State quantity curve of double pendulum bridge crane system with two switching functions.

(2) To compare and analyze VP-TVSMC, CSMC method and PDSMC method.

In this paper, three kinds of external interference are designed and simulated. In the simulation process, the following interferences are artificially added to affect the load swing angle:

1) A sine wave interference with a relative amplitude of 25% and a frequency of 0.5Hz is added between 12 and 14 seconds.
2) A pulse jamming with a relative amplitude of 25% and a pulse width of 0.5 seconds is added between 19 and 19.5 seconds.
3) A random disturbance of 25% relative amplitude is added between 24 and 26 seconds.

Among these interferences, the relative amplitude is defined as the percentage ratio between the amplitude of pendulum angle interference and the maximum amplitude of load swing in the whole process. The simulation experiment results are shown in Fig.7, in which Fig.7(a) pertains to be the disturbance sequence diagram.

From Figs. 7(b)-(f) we can see that under the control of VP-TVSMC and CSMC, the trolley can still reach the desired position accurately within a very short period of time, and both the first and second swing angles can be limited within

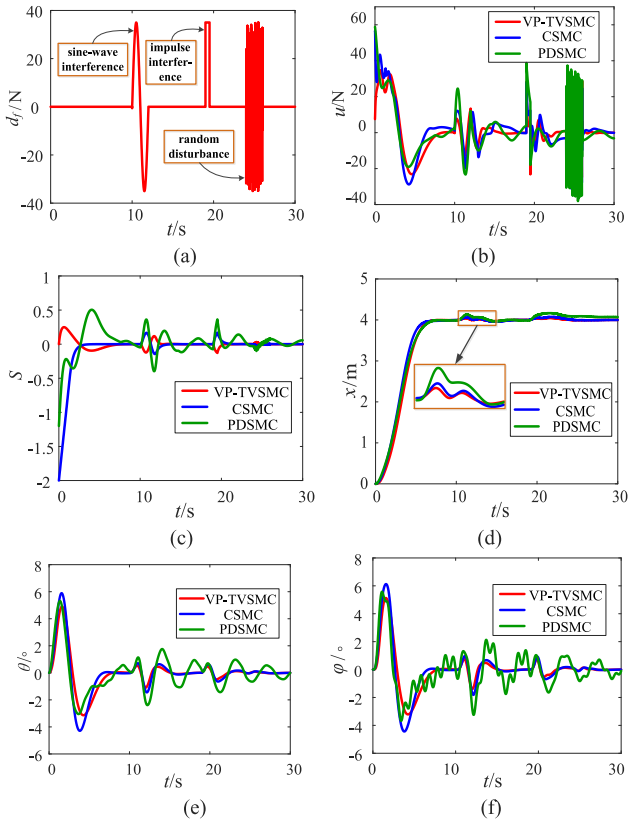

FIGURE 7. The state quantity curve of double pendulum bridge crane system under three kinds of disturbances.

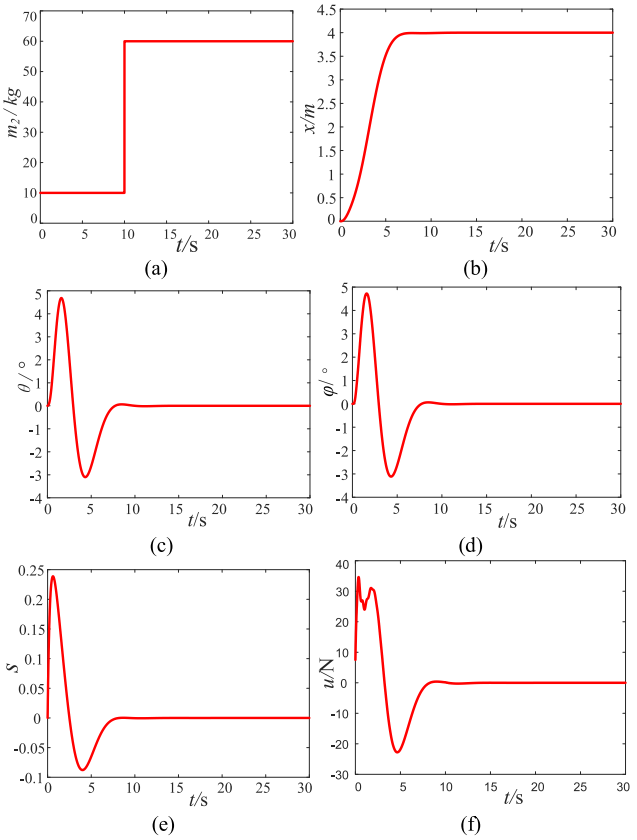

FIGURE 8. State quantity curve in variable mass double pendulum bridge crane system.

a reasonable range. The difference is that under the control of PDSMC, the positioning of the trolley has been offset, and the swing angle has also been buffeted violently. It is worth noting that all three external disturbances are barely sensitive to the trolley displacement of VP-TVSMC and CSMC. Under the action of the two controllers, the first swing angle and the second swing angle can quickly converge to 0°, and it has a great influence on the trolley positioning and load anti-swing of PDSMC. It can be clearly acknowledged that the influence of sinusoidal interference on the swing angle is the largest, followed by impulse interference and the influence of random interference subsequently. Afterwards, it can be found that the interference result for the sliding surface shares low similarities with that for swing angle. When the driving force of the trolley is disturbed, the controller can also react quickly to restrain the change of system state and control the driving force to zero quickly. Conversely, the influence of sine wave interference on the driving force is the least, followed by pulse interference, and the influence of random interference.

Taking all the interference inhibition effect of Figs.7(b)-(f) into consideration, it can be concluded that the proposed VP-TVSMC in this paper features with high positioning accuracy and more significant inhibition effect than CSMC method and PDSMC method, which are appreciated in practical application. Since inevitable external interference will not vanish completely and possibly becomes even more rampant compared to the factors existing in the experiments, the control method proposed in this paper enjoys a more than high value.

Experiment 4: The payload mass is changed to verify the robustness of the proposed control approach against parametric uncertainties. When $t = 10$ s, the load mass m_p is suddenly changed from 10kg to 60kg, while the hook mass m_1 remains still 2kg and the control gain stays the same as that in Table 1 with VP-TVSMC adopted as the controller.

Experiment 5: When $t = 10$ s, the connecting rope length l_2 between the hook and the load is suddenly changed from 0.3m to 1.8m, while the connecting rope length l_1 between the trolley and the hook still remains as 1 m and the control gain stays the same as that in Table 1 with VP-TVSMC adopted as the controller.

Fig. 8 and Fig. 9 show the simulation results of the VP-TVSMC method regarding to uncertainty and mutation of load mass and the length of the hook and load connection rope, from which it can be acknowledged that the designed controller can achieve better control performance even under uncertain system parameters. In conclusion, the VP-TVSMC method proposed in this paper displays better performance and strong robustness against external disturbances and indefinite system parameters (such as load mass change and the

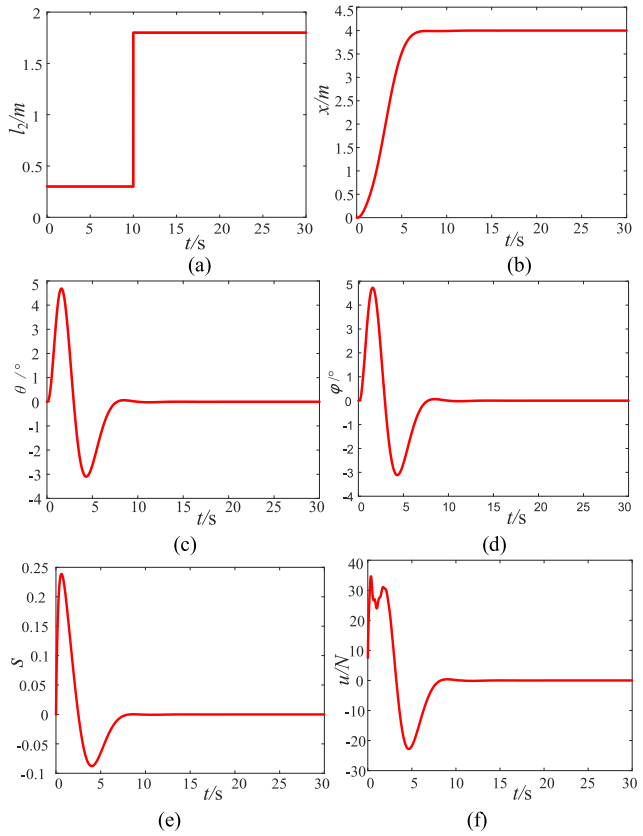

FIGURE 9. The state quantity curve of double pendulum bridge crane system with variable rope length.

connecting rope length change between the hook and the load).

V. CONCLUSION

In order to realize the anti-swing suppression and precise positioning of the distributed mass double pendulum bridge crane system, the VP-TVSMC designed in this paper can effectively eliminate the sliding mode control to reach the motion stage, realize the dynamic adjustment of sliding mode parameters, and ensure the system robustness in whole response process. However, trolley likewise features with a lot of uncertainties in the process of transportation. Hence, this paper set up three kinds of interference factors such as sine wave interference, pulse interference and random disturbance, and uncertain system parameters to not only test the control performance of VP-TVSMC and the stability of the system but also verify stabilization performance of vibration of the proposed continuous function of th(S) towards VP-TVSMC. Afterwards relevant simulation experiments have been conducted with their results to prove that VP-TVSMC provides a rapid response to positioning, shows good swing suppression performance and strong robustness to external interference and the continuous function th(S) enjoys a favourable effect on anti-chattering. In the follow-up work, we will devote more efforts to improving the adaptability of this method to other underactuated control system, such as casting crane system and inverted pendulum system.

REFERENCES

[1] B. Yang, Z.-X. Liu, H.-K. Liu, Y. Li, and S. Lin, "A GPC-based multivariable PID control algorithm and its application in anti-swing control and accurate positioning control for bridge cranes," *Int. J. Control, Autom. Syst.*, vol. 18, no. 10, pp. 2522–2533, Oct. 2020.

[2] D. Chwa, "Sliding-mode-control-based robust finite-time antisway tracking control of 3-D overhead cranes," *IEEE Trans. Ind. Electron.*, vol. 64, no. 8, pp. 6775–6784, Aug. 2017.

[3] I. Shah and F. U. Rehman, "Smooth second order sliding mode control of a class of underactuated mechanical systems," *IEEE Access*, vol. 6, pp. 7759–7771, Feb. 2018.

[4] Y. Wang, N. Sun, Y. Wu, X. Chen, and Y. Fang, "Point-to-point motion control for flexible crane systems working in the deep sea," *Meas. Control*, vol. 53, nos. 7–8, pp. 1041–1048, Aug. 2020.

[5] Z. Sun, Y. Bi, X. Zhao, Z. Sun, C. Ying, and S. Tan, "Type-2 fuzzy sliding mode anti-swing controller design and optimization for overhead crane," *IEEE Access*, vol. 6, pp. 51931–51938, Sep. 2018.

[6] K. Ammari and B. Chentouf, "Further results on the long-time behavior of a 2D overhead crane with a boundary delay: Exponential convergence," *Appl. Math. Comput.*, vol. 365, pp. 1–17, Jan. 2020.

[7] N. Sun, J. Zhang, X. Xin, T. Yang, and Y. Fang, "Nonlinear output feedback control of flexible rope crane systems with state constraints," *IEEE Access*, vol. 7, pp. 136193–136202, Sep. 2019.

[8] Q. Wu, X. Wan, and L. Hua, "Dynamic analysis and time optimal anti-swing control of double pendulum bridge crane with distributed mass beams," *Mech. Syst. Signal Process.*, vol. 144, pp. 1–20, Oct. 2020.

[9] X. Xing and J. Liu, "PDE modelling and vibration control of overhead crane bridge with unknown control directions and parametric uncertainties," *IET Control Theory Appl.*, vol. 14, no. 1, pp. 116–126, Jan. 2020.

[10] M. J. Maghsoudi, L. Ramli, S. Sudin, Z. Mohamed, A. R. Husain, and H. Wahid, "Improved unity magnitude input shaping scheme for sway control of an underactuated 3D overhead crane with hoisting," *Mech. Syst. Signal Process.*, vol. 123, pp. 466–482, May 2019.

[11] M. J. Maghsoudi, Z. Mohamed, S. Sudin, S. Buyamin, H. I. Jaafar, and S. M. Ahmad, "An improved input shaping design for an efficient sway control of a nonlinear 3D overhead crane with friction," *Mech. Syst. Signal Process.*, vol. 92, pp. 364–378, Aug. 2017.

[12] N. Sun, Y. Wu, H. Chen, and Y. Fang, "An energy-optimal solution for transportation control of cranes with double pendulum dynamics: Design and experiments," *Mech. Syst. Signal Process.*, vol. 102, pp. 87–101, Mar. 2018.

[13] H. Chen, Y. Fang, and N. Sun, "A time-optimal trajectory planning strategy for double pendulum cranes with swing suppression," in *Proc. 35th Chin. Control Conf. (CCC)*, Jul. 2016, pp. 4599–4604.

[14] M. Zhang, Y. Zhang, and X. Cheng, "Finite-time trajectory tracking control for overhead crane systems subject to unknown disturbances," *IEEE Access*, vol. 7, pp. 55974–55982, Apr. 2019.

[15] K. Matsusawa, Y. Noda, and A. Kaneshige, "On-demand trajectory planning with load sway suppression and obstacles avoidance in automated overhead traveling crane system," in *Proc. IEEE 15th Int. Conf. Automat. Sci. Eng. (CASE)*, Aug. 2019, pp. 1321–1326.

[16] N. Sun, T. Yang, Y. Fang, Y. Wu, and H. Chen, "Transportation control of double-pendulum cranes with a nonlinear quasi-PID scheme: Design and experiments," *IEEE Trans. Syst., Man, Cybern. Syst.*, vol. 49, no. 7, pp. 1408–1418, Jul. 2019.

[17] B. Lu, Y. C. Fang, and N. Sun, "Adaptive output-feedback control for dual overhead crane system with enhanced anti-swing performance," *IEEE Trans. Control Syst. Technol.*, vol. 22, no. 7, pp. 1–14, Aug. 2019.

[18] G.-H. Kim and K.-S. Hong, "Adaptive sliding-mode control of an offshore container crane with unknown disturbances," *IEEE/ASME Trans. Mechatronics*, vol. 24, no. 6, pp. 2850–2861, Dec. 2019.

[19] L. A. Tuan and S.-G. Lee, "Sliding mode controls of double-pendulum crane systems," *J. Mech. Sci. Technol.*, vol. 27, no. 6, pp. 1863–1873, Jun. 2013.

[20] M. Zhang, Y. Zhang, and X. Cheng, "An enhanced coupling PD with sliding mode control method for underactuated double-pendulum overhead crane systems," *Int. J. Control, Autom. Syst.*, vol. 17, no. 6, pp. 1579–1588, May 2019.

[21] L. Xue, G. Zhiyong, and P. XiuHui, "A double-sliding surface based control method for underactuated cranes," in *Proc. 37th Chin. Control Conf. (CCC)*, Jul. 2018, pp. 1768–1934.

[22] Y. Wang, O. A. Postolache, W. Xu, S. Ye, D. Ni, and M. Zhong, "Fuzzy sliding mode synchronous control of double-container for overhead crane," in *Proc. 11th Int. Symp. Adv. Topics Electr. Eng. (ATEE)*, Mar. 2019, pp. 1–7.
[23] X. Wu and X. He, "Nonlinear energy-based regulation control of three-dimensional overhead cranes," *IEEE Trans. Autom. Sci. Eng.*, vol. 14, no. 2, pp. 1297–1308, Apr. 2017.
[24] M. Shi, S. Guo, L. Jiang, and Z. Huang, "Active-passive combined control system in crane type for heave compensation," *IEEE Access*, vol. 7, pp. 159960–159970, Oct. 2019.
[25] H. Chen, Y. Fang, and N. Sun, "A swing constrained time-optimal trajectory planning strategy for double pendulum crane systems," *Nonlinear Dyn.*, vol. 89, no. 2, pp. 1513–1524, Apr. 2017.
[26] M. Zhang, X. Ma, H. Chai, X. Rong, X. Tian, and Y. Li, "A novel online motion planning method for double-pendulum overhead cranes," *Nonlinear Dyn.*, vol. 85, no. 2, pp. 1079–1090, Mar. 2016.
[27] M. Zhang, X. Ma, R. Song, X. Rong, G. Tian, X. Tian, and Y. Li, "Adaptive proportional-derivative sliding mode control law with improved transient performance for underactuated overhead crane systems," *IEEE/CAA J. Autom. Sinica*, vol. 5, no. 3, pp. 683–690, May 2018.

TIANLEI WANG received the B.S.E. degree in electrical engineering from the Beijing University of Posts and Telecommunications, and the M.S. degree in signal processing from the South China University of technology. He is currently pursuing the Ph.D. degree with Beijing Jiaotong University. His research interests include intelligent systems, control theory, and pattern recognition.

NANLIN TAN is currently a Professor and a Ph.D. Supervisor with Beijing Jiaotong University, Beijing, China. His research interests include safety technology engineering, control theory, and pattern recognition.

XIANWEN ZHANG was born in Qingyuan, Guangdong, China, in December 1997. He is currently pursuing the bachelor's degree in traffic engineering with the Intelligent Manufacturing Department, Wuyi University. His main research interests include underdrive system modeling and nonlinear control.

GUOZHENG LI received the B.S. degree in detection technique and instrument and the Ph.D. degree from Beijing Jiaotong University, Beijing, China, in 2005 and 2014, respectively. He is currently an Associate Professor with the School of Mechanical, Electronic and Control Engineering, Beijing Jiaotong University. His research interests include the design of the control, monitoring and diagnosis system of rail transit vehicles, signal processing technology, and multi-scenario applications of artificial intelligence in vehicle-ground collaboration.

SHUQIANG SU was born in Qinghai, China, in 1971. He received the B.S. degree from the Department of Mechanical Engineering, Beijing Jiaotong University, in 1992, and the Ph.D. degree from the School of Mechanical, Electronic and Control Engineering, Beijing Jiaotong University, in 2017. He is currently a Lecturer with the School of Mechanical, Electronic and Control Engineering, Beijing Jiaotong University. His research interests include application of magnetic liquid, new sensor, and measurement and control technology.

JING ZHOU was born in Ji'an, Jiangxi, China, in November 1997. He is currently pursuing the master's degree in mechanical engineering with the Intelligent Manufacturing Department, Wuyi University. His main research interests include underdrive system modeling and nonlinear control.

JIONGZHI QIU was born in Lufeng, Guangdong, China, in December 1999. He is currently pursuing the bachelor's degree in traffic engineering with the Intelligent Manufacturing Department, Wuyi University. His main research interests include underdrive system modeling and nonlinear control.

ZHIQIN WU was born in Ganzhou, Jiangxi, China, in December 1999. She is currently pursuing the bachelor's degree in mathematics and applied mathematics with the Department of Mathematics and Computational Sciences, Wuyi University. Her main research interests include underdrive system modeling and nonlinear control.

YIKUI ZHAI (Member, IEEE) received the bachelor's degree in optical electronics information and communication engineering and the master's degree in signal and information processing from Shantou University, Guangdong, China, in 2004 and 2007, respectively, and the Ph.D. degree in signal and information processing with Beihang University, in June 2013. Since October 2007, he has been working with the Department of Intelligence Manufacturing, Wuyi University, Guangdong, China. From June 2016 to June 2017, he was a Visiting Scholar with the Department of Computer Science, University of Milan. He is currently an Associate Professor with Wuyi University, Guangdong, China. His research interests include: image processing, biometric extraction, deep learning, and pattern recognition.

RUGGERO DONIDA LABATI (Member, IEEE) received the Ph.D. degree in computer science from the Universitá degli Studi di Milano, Crema, Italy, in 2013. Since 2015, he has been an Assistant Professor of computer science with the Universitá degli Studi di Milano. He has been a Visiting Researcher with Michigan State University, East Lansing, MI, USA. Original results have been published in more than 50 articles in international journals, proceedings of international conferences, books, and book chapters. His current research interests include intelligent systems, signal and image processing, machine learning, pattern analysis and recognition, theory and industrial applications of neural networks, biometrics, and industrial applications. He is an Associate Editor of the *Journal of Ambient Intelligence and Humanized Computing* (Springer).

VINCENZO PIURI (Fellow, IEEE) received the M.S. and Ph.D. degrees in computer engineering from the Politecnico di Milano, Italy. He was an Associate Professor with the Politecnico di Milano, Italy, from 1992 to 2000, a Visiting Professor with The University of Texas at Austin, USA, from 1996 to 1999, and a Visiting Researcher with George Mason University, USA, from 2012 to 2016. Since 2000, he has been a Full Professor with the University of Milan, Italy. From 2007 to 2012, he was also the Department Chair. He founded a start-up company, Sensure srl, in the area of intelligent systems for industrial applications (leading it from 2007 to 2010). He was active in industrial research projects with several companies. His main research interests include intelligent systems, computational intelligence, pattern analysis and recognition, machine learning, signal and image processing, biometrics, intelligent measurement systems, industrial applications, distributed processing systems, the Internet-of-Things, cloud computing, fault tolerance, application-specific digital processing architectures, and arithmetic architectures. He is an ACM Fellow.

FABIO SCOTTI (Member, IEEE) received the Ph.D. degree in computer engineering from the Politecnico di Milano, Milan, Italy, in 2003. Since 2015, he has been an Associate Professor of computer science with the Universitá degli Studi di Milano, Crema, Italy. Original results have been published in more than 100 articles in international journals, proceedings of international conferences, books, book chapters, and patents. His current research interests include biometric systems, machine learning and computational intelligence, signal and image processing, theory and applications of neural networks, three-dimensional reconstruction, industrial applications, intelligent measurement systems, and high-level system design. He is an Associate Editor of the IEEE TRANSACTIONS ON HUMAN-MACHINE SYSTEMS and *Soft Computing* (Springer).